ISSN 1674-1056
http://cpb.iphy.ac.cn
http://iopscience.iop.org/cpb
中国物理 B
Chinese Physics
中国物理 Chinese Physics B

Precisely tuning Ge substitution for efficient solution-processed $Cu_2ZnSn(S, Se)_4$ solar cells

Xinshou Wang(王新收), Dongxing Kou(寇东星), Wenhui Zhou(周文辉), Zhengji Zhou(周正基), Qingwen Tian(田庆文), Yuena Meng(孟月娜), Sixin Wu(武四新)
Citation: Chin. Phys. B . 2018, 27(1): 018809. **doi:** 10.1088/1674-1056/27/1/018809

Journal homepage: http://cpb.iphy.ac.cn; http://iopscience.iop.org/cpb

What follows is a list of articles you may be interested in

Importance of PbI_2 morphology in two-step deposition of $CH_3NH_3PbI_3$ for high-performance perovskite solar cells

Hui Wei(韦慧), Yang Tang(汤洋), Bo Feng(冯波), Hui You(尤晖)
Chin. Phys. B . 2017, 26(12): 128801. **doi:** 10.1088/1674-1056/26/12/128801

Improvement in IBC-silicon solar cell performance by insertion of highly doped crystalline layer at heterojunction interfaces

Hadi Bashiri, Mohammad Azim Karami, Shahramm Mohammadnejad
Chin. Phys. B . 2017, 26(10): 108801. **doi:** 10.1088/1674-1056/26/10/108801

Influence of interface states, conduction band offset, and front contact on the performance of a-SiC: H(n)/c-Si(p) heterojunction solar cells

Zhi Qiao(乔治), Jian-Li Ji(冀建利), Yan-Li Zhang(张彦立), Hu Liu(刘虎), Tong-Kai Li(李同锴)
Chin. Phys. B . 2017, 26(6): 068802. **doi:** 10.1088/1674-1056/26/6/068802

O_3 fast and simple treatment-enhanced p-doped in Spiro-MeOTAD for CH_3NH_3I vapor-assisted processed $CH_3NH_3PbI_3$ perovskite solar cells

En-Dong Jia(贾恩东), Xi Lou(娄茜), Chun-Lan Zhou(周春兰), Wei-Chang Hao(郝维昌), Wen-Jing Wang(王文静)
Chin. Phys. B . 2017, 26(6): 068803. **doi:** 10.1088/1674-1056/26/6/068803

Simulation design of P-I-N-type all-perovskite solar cells with high efficiency

Hui-Jing Du(杜会静), Wei-Chao Wang(王韦超), Yi-Fan Gu(顾一帆)
Chin. Phys. B . 2017, 26(2): 028803. **doi:** 10.1088/1674-1056/26/2/028803

SPECIAL TOPIC — New generation solar cells

Precisely tuning Ge substitution for efficient solution-processed $Cu_2ZnSn(S, Se)_4$ solar cells*

Xinshou Wang(王新收), Dongxing Kou(寇东星)†, Wenhui Zhou(周文辉), Zhengji Zhou(周正基), Qingwen Tian(田庆文), Yuena Meng(孟月娜), and Sixin Wu(武四新)‡

The Key Laboratory for Special Functional Materials of MOE, Collaborative Innovation Center of Nano Functional Materials and Applications, Henan University, Kaifeng 475004, *China*

(Received 28 September 2017; revised manuscript received 17 November 2017; published 22 December 2017)

The kesterite $Cu_2ZnSn(S,Se)_4$ (CZTSSe) solar cells have yielded a prospective conversion efficiency among all thin-film photovoltaic technology. However, its further development is still hindered by the lower open-circuit voltage (V_{oc}), and the non-ideal bandgap of the absorber is an important factor affecting this issue. The substitution of Sn with Ge provides a unique ability to engineer the bandgap of the absorber film. Herein, a simple precursor solution approach was successfully developed to fabricate $Cu_2Zn(Sn_yGe_{1-y})(S_xSe_{1-x})_4$ (CZTGSSe) solar cells. By precisely adjusting the Ge content in a small range, the V_{oc} and J_{sc} are enhanced simultaneously. Benefitting from the optimized bandgap and the maintained spike structure and light absorption, the 10% Ge/(Ge+Sn) content device with a bandgap of approximately 1.1 eV yields the highest efficiency of 9.36%. This further indicates that a precisely controlled Ge content could further improve the cell performance for efficient CZTGSSe solar cells.

Keywords: $Cu_2ZnSn(S,Se)_4$, solar cells, Ge substitution, bandgap

PACS: 88.40.ff, 88.40.hj, 88.40.jn, 85.60.Bt **DOI:** 10.1088/1674-1056/27/1/018809

1. Introduction

As a promising material for the next-generation thin-film solar cells, $Cu(In,Ga)Se_2$ (CIGS) has received great attention owing to its earth-abundant components, low toxicity, high adsorption coefficient, good stability, etc.[1] However, owing to the scarcity of In and Ga, the large-scale utilization of CIGS remains challenging. The substitution of In and Ga with earth-abundant Zn and Sn to prepare $Cu_2ZnSn(S_xSe_{1-x})_4$ (CZTSSe) has emerged as an attractive strategy toward the practical application of thin-film solar cells. In the past few decades, a large number of methods have been applied to fabricate CZTSSe solar cells, such as magnetron sputtering,[2,3] thermal evaporation,[4–7] precursor solution approach,[8–12] nanocrystal solution process,[13–16] and electrodeposition method.[17–19] To date, the precursor solution approach has been considered as a prospective route to achieve high efficiency and the hydrazine precursor solution-based CZTSSe cells have achieved the highest efficiency of 12.6%,[10] which is still far from the record efficiency of CIGS cells (22.3%).

Many researches have demonstrated that the defective efficiency of CZTSSe solar cells is mainly ascribed to its lower open-circuit voltage (V_{oc}), and the narrow bandgap of the CZTSSe layer is an important factor responsible for this issue. Appropriately increasing the optical bandgap of the absorber is critical for improving the performance of thin-film solar cells. In CIGSe solar cells, the substitution of 25%–30% of In by Ga is typically employed to enhance the V_{oc}.[1] For the CZTSSe system, similar bandgap tuning of absorber layer by adjusting the Ge/(Ge+Sn) ratio has also been expected as a promising route to improve the device performance.[20–25] In 2016, Hill house prepared CZTGSSe thin-film solar cells by dissolving metal chlorides using DMF as the solvent, and achieved the record efficiency of 11%.[25] The precursor solution processing approach has been proven to be more effective to achieve high efficiency rather than nanoparticle-based deposition approaches. However, most Ge tuning in previous literature were usually in the range 0–100%. Although this wide range could increase the bandgap of the absorber dramatically, the narrow light harvesting range will limit the short-circuit current density (J_{sc}). Furthermore, the conduction band edge of CZTGSSe film shifts to the higher energy level than that of the CdS buffer layer and a cliff structure is formed, which is also harmful to the performance enhancement, owing to the increased electron–hole recombination. As a result, the high-V_{oc} Ge-substituted CZTGSSe devices often exhibit lower J_{sc}, which cannot effectively improve cell performance, and pre-

*Project supported by the Joint Talent Cultivation Funds of NSFC-HN (Grant No. U1604138), the National Natural Science Foundation of China (Grant Nos. 21603058 and 51702085), the Innovation Research Team of Science and Technology in Henan Province, China (Grant No. 17IRTSTHN028), the Science and Technology Innovation Talents in Universities of Henan Province, China (Grant No. 18HASTIT016), and the Young Key Teacher Foundation of Universities of Henan Province, China (Grant No. 2015GGJS-022).

†Corresponding author. E-mail: koudongxing@henu.edu.cn

‡Corresponding author. E-mail: wusixin@henu.edu.cn

© 2018 Chinese Physical Society and IOP Publishing Ltd

cise tuning of Ge is urgently needed.

Herein, a simple precursor solution process was developed to prepare CZTGSSe thin film by dissolving GeO_2 into CZTSSe precursor solution (Cu, Zn, Sn, S, and Se in ethylenediamine and dithioglycol). The advantage of this green approach is that there are no additional surfactants and impurity atoms present. X-ray diffraction (XRD) and Raman characterizations indicate that Sn is partly substituted by Ge. By precisely adjusting the Ge content in a small range (0–50 at.%), the spike structure and light absorption were maintained well and the V_{oc} and J_{sc} were enhanced simultaneously. Finally, the 10% Ge content device with a bandgap of approximately 1.1 eV yields the best conversion efficiency of 9.36%.

2. Experimental section

2.1. Materials

Cu (99.9%), Zn (99.9%), GeO_2 (99.99%), and S (99.9%) powders were purchased from Aladdin. Sn (99.8%), Se (99%), 1,2-ethanedithiol ($C_2H_6S_2$, AR), 1,2-ethylenediamine ($C_2H_6N_2$, AR), thioglycolic acid ($C_2H_4O_2S$, AR), ethanolamine (C_2H_7NO, AR), 2-methoxyethanol ($C_3H_8O_2$, AR), ammonium hydroxide (NH_4OH, 25%), cadmium sulfate (AR) and thiourea (AR) were furnished by Alfa Aesar. All chemicals and reagents were commercially available and used as received without further purification.

2.2. Preparation of CZTGSSe precursor solution

Cu–Zn–Sn–S–Se solution was prepared by dissolving Cu, Zn, Sn, S, and Se in the mixture of ethanediamine and dithioglycol. Typically, 1.24 mmol Cu, 0.76 mmol Zn, x mmol Sn ($x = 0.71$, 0.674, 0.639, 0.568, 0.497, and 0.355), 2.7 mmol S and 0.3 mmol Se were placed into 25 mL round flasks, followed by 5 ml ethanediamine and 0.5 ml dithioglycol added in. The mixtures were kept at 70 °C under vigorous stirring until the solution became transparent (approximately 1.5 h).

Ge solution was prepared by dissolving y mmol GeO_2 ($y = 0$, 0.108, 0.213, 0.426, 0.639, and 1.065) in a mixture of 0.75 mL thioglycolic acid, 0.75 mL ethanolamine and 1.5 mL 2-methoxyethanol. The mixtures were also kept at 70 °C under vigorous stirring until GeO_2 was completely dissolved (approximately 1.5 h).

To prepare CZTGSSe precursor solution, 1 mL Ge solution was added into Cu–Zn–Sn–S–Se solution and then stirred at 70 °C for 30 min. Different ratios of Ge/(Sn+Ge) (0%, 5%, 10%, 20%, 30%, and 50%) precursor solution were obtained.

2.3. Fabrication of CZTGSSe thin-film solar cells

CZTGSSe precursor films were prepared by spin coating of metal precursor solutions on molybdenum sputtered soda lime glass (SLG) and then heating on a hot plate at 310 °C in nitrogen atmosphere for 1 min. A thickness of about 1.7 mm thin film was obtained by repeating the procedure several times. Finally, the thin film was annealed at 550 °C in a graphite box containing 200 mg of Se powder for 15 min. CZTGSSe films were further deposited with 60 nm cadmium sulfide (CdS) via chemical bath deposition (CBD), 70 nm sputtering intrinsic zinc oxide (ZnO), 200 nm indium-doped tin oxide (ITO) successively. On the top of the device, Ag collection grid electrodes were deposited by thermal evaporation.

2.4. Characterizations

Powder XRD measurements were performed on a Bruker D8 Advance x-ray diffractometer. Raman spectra were measured using a Raman microscope with an excitation laser at 532 nm. Scanning electron microscopy (SEM) images were recorded using a Nova NanoSEM 450 field emission scanning electron microscope (FESEM). Photocurrent density–voltage curves were collected with a Keithley 2400 source meter under AM 1.5G illumination (100 mW·cm^{-2}). External quantum efficiency (EQE) spectra were measured using a Zolix SCS100 QE system equipped with a 150-W xenon light source and a lock-in amplifier.

3. Results and discussion

Figure 1 shows XRD patterns of CZTGSSe with different ratios of Ge/(Sn+Ge). The peaks located at 27.5°, 45.5°, and 54.1° could be assigned, respectively, to the (112), (204), and (312) lattice planes of kesterite CZTGSSe, whereas the peak at 40.4° is attributed to the back electrode of Mo. Comparing with that of CZTSSe (JCPDS, No. 52-0868), the (112) diffraction peaks of CZTGSSe increase gradually with increasing Ge content, as seen in Fig. 1(b). The replacement of larger Sn atom by smaller Ge atom decreases the lattice constant and thus shifts the XRD diffraction peaks to a larger degree. Based on the XRD analysis, it could be concluded the Ge atoms entered the lattice and CZTGSSe film was successfully prepared.

However, the XRD results alone could not exclude the impurities, such as the secondary phases of ZnSe and Cu_2SnSe_3, and thus Raman spectra were obtained. Figure 2 illustrates the Raman spectra of CZTGeSSe films with different Ge content. Four peaks were observed, where the 172, 196, and 234 cm^{-1} peaks are assigned to the A1 mode of bulk CZTSe and the 328 cm^{-1} peak corresponds to the bulk CZTS. No other observable peaks suggest pure-phase CZTGSSe films are formed. Figure 2(b) presents the Raman spectra between 150 and 250 cm^{-1}, and typical peaks move to a higher wavenumber with increasing Ge content, which is in accordance with the previous report.[27]

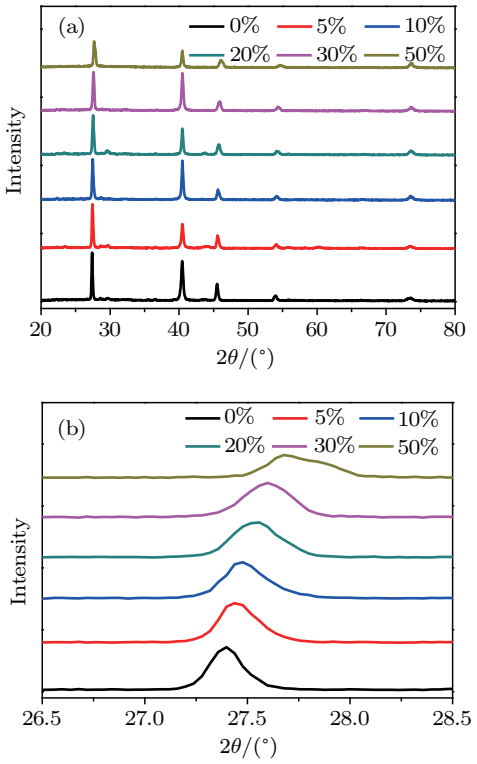


Fig. 1. (color online) (a) XRD patterns and (b) enlarged (112) crystal face of CZTGSSe films with different Ge content.

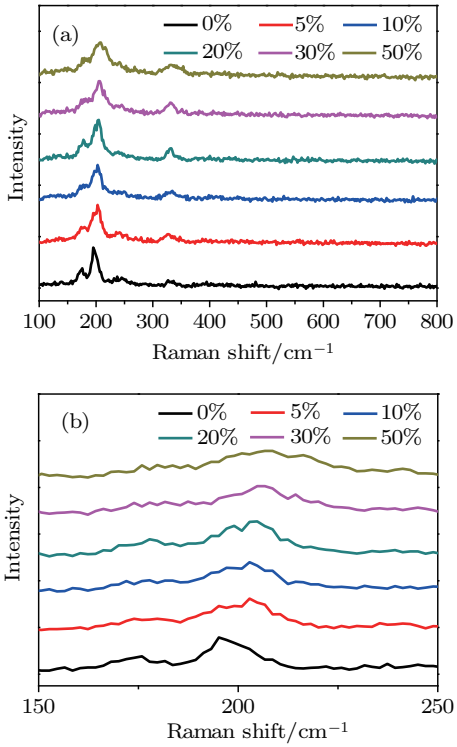


Fig. 2. (color online) (a) Raman spectra and (b) enlarged Se atom peaks of CZTGSSe films with different Ge content.

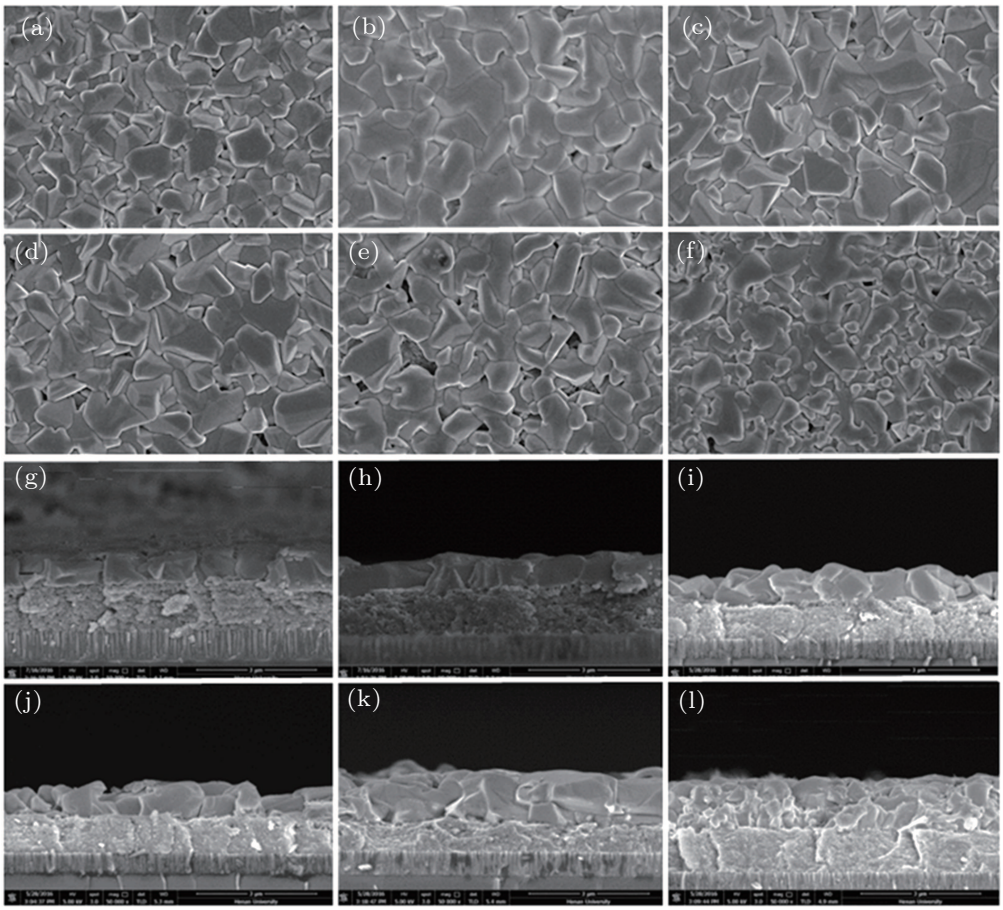


Fig. 3. Top view (a)–(f) and cross-section (g)–(l) SEM images of CZTGSSe with different Ge content of 0%, 5%, 10%, 20%, 30%, and 50%. Scale bar: 3 μm.

Figure 3 shows SEM images of CZTGSSe with different amounts of Ge. From the top-view images, it can be found that no difference in the surface morphology is observed when the amount of Ge is lower than 20%, and all the samples are generally composed with compact large grains. When the amount of Ge reaches 30%, some voids appear and this morphology will cause electric leakage and decrease the cell performance.[28] However, the cross-section morphology implies that the crystallization and grain size are both enhanced with increasing Ge content (0–30%). Table 1 lists the actual elemental contents in CZTGSSe detected by EDX. The Cu/(Zn+Sn+Ge) and Zn/(Sn+Ge) ratios are remarkably increased with increasing Ge content, which is mainly attributed to the loss of Ge in the selenization process at high temperature via formation of $GeSe_2$ gas. It could also be observed that the Ge loss amount increases with increasing Ge content. For instance, when the addition amount is 50%, the Ge loss amount is nearly to 50%. This large Ge loss amount will be responsible for the worse crystallinity of CZTGSSe films at high substitution content.

Table 1. EDX data of the selenized CZTGSSe films with different Ge content.

Sample/%	Cu/%	Zn/%	Ge/%	Sn/%	S/%	Se/%	Cu/(Zn+Ge+Sn)	Zn/(Ge+Sn)	Ge/(Zn+Ge)
0	18.82	11.67	0	9.35	10.76	49.60	0.895	1.248	0
5	18.83	11.70	0.32	8.87	11.25	49.03	0.901	1.273	0.035
10	18.83	11.75	0.72	8.42	11.20	49.08	0.902	1.286	0.079
20	18.86	11.80	1.52	7.57	11.09	49.14	0.902	1.297	0.167
30	19.29	12.05	1.61	6.82	11.06	49.18	0.942	1.429	0.191
50	19.75	12.85	1.92	5.24	11.04	49.20	0.987	1.794	0.268

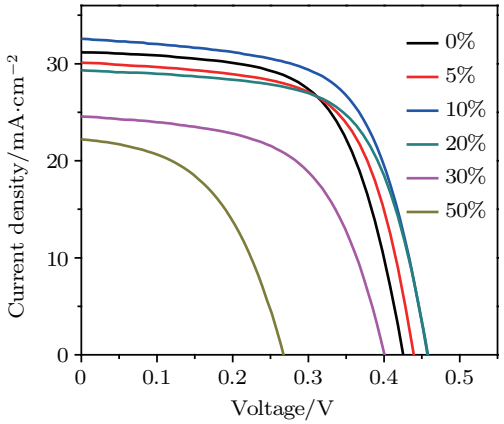


Fig. 4. (color online) *J*–*V* curves of CZTGSSe solar cells with different Ge content.

The Ge-substituted CZTGSSe films were directly employed as absorber layers for solar cells with the structure of Ag/ITO/*i*-ZnO/CdS/ CZTGSSe/Mo/glass. Figure 4 shows *J*–*V* curves of CZTGSSe solar cells with different Ge content under AM 1.5 G illumination. The detailed parameters for the CZTGSSe thin-film solar cells are also listed in Table 2. It can be found that the efficiency for CZTGSSe solar cells increases firstly and then decreases with increasing Ge content. The 10% Ge content device achieves the champion efficiency of 9.36%, with the V_{oc} of 0.457 V, J_{sc} of 32.6 mA·cm^2, and FF of 63.0%, respectively. A precisely adjusted Ge amount in the range of 0–20% can enhance V_{oc} and J_{sc} simultaneously, mainly due to the enlarged bandgap and the maintained light absorption. When the Ge content increases to 30%, a more negative shift in the conduction band edge for CZTGSSe films will transfer the spike structure into cliff structure at ZnO/CdS/CZTGSSe heterojunction, accompanied with larger recombination. Additionally, the light absorption and crystallinity will become worse at high Ge content. Both the above issues decrease V_{oc} and J_{sc} dramatically and only the 10% device could improve cell performance, and this value is far from the previous reported (40%).

Table 2. Detailed performance parameters of CZTGSSe solar cells with different Ge content.

Device	Eff/%	V_{oc}/V	J_{sc}/mA·cm^{-2}	FF/%	R_s/Ω·cm^{-2}	R_{sh}/Ω·cm^{-2}
0 %	8.31	0.425	31.19	62.74	10.90	1499.97
5%	8.45	0.438	30.08	64.12	9.88	1212.15
10%	9.36	0.457	32.55	62.97	10.20	934.84
20%	8.63	0.457	29.29	64.41	10.95	1472.15
30%	5.68	0.400	24.53	57.84	14.73	927.94
50%	2.90	0.267	22.14	49.00	16.55	517.86

Figure 5 depicts the EQE curves of CZTGSSe solar cells with Ge/(Sn+Ge) ratios of 0.0, 0.05, 0.1, 0.2, and 0.3. The bandgap is typically estimated from linear extrapolation of the EQE data with respect to photon energy. The EQE measurements are carried out in DC mode and the data of the 50% Ge content device cannot be detected, which might be ascribed to the electric leakage and partial short circuit. As shown in Fig. 5, the EQE gradually decreases with increasing Ge content in the range of 10%–30%, as well as the tendency of J_{sc}. The bandgap of CZTGSSe films increases from 1.04 eV to 1.20 eV with increasing Ge content and the 10% content device achieves the optimal value of 1.1 eV for efficient photovoltaic solar cells. This result also indicates that precisely tuning the Ge content in a small range is more favorable for CZTGSSe devices.

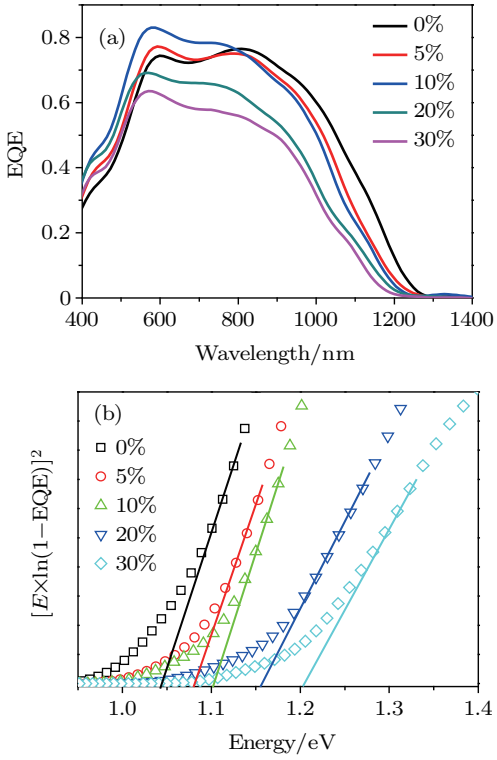


Fig. 5. (color online) (a) EQE curves and (b) the estimated bandgap of CZTGSSe solar cells with different Ge/(Sn+Ge) ratios.

4. Conclusion and perspectives

In summary, a simple precursor solution approach was successfully performed to fabricate CZTGSSe solar cells. By precisely adjusting the Ge content in a small range, the V_{oc} and J_{sc} are enhanced simultaneously, owing to the enlarged bandgap and the maintained spike structure and light absorption. However, when the Ge substitution content increases to 30%, the electric leakage and partial short-circuit would reduce cell performance dramatically. Finally, the 10% Ge content device achieves the highest efficiency of 9.36%. Different from previous report, this precisely controlled Ge content offers a new aspect: that the band alignment and light absorption should also be considered for future V_{oc} enhancement research of CZTSSe solar cells.

References

[1] Qi Y F, Kou D X, Zhou W H, Zhou Z J, Tian Q W, Meng Y N, Liu X S, Du Z L and Wu S X 2017 *Energy Environ. Sci.* **10** 2401
[2] Jimbo K, Kimura R, Kamimura T, Yamada S, Maw W S, Araki H, Oishi K and Katagiri H 2007 *Thin Solid Films* **515** 5997
[3] Yang K J, Son D H, Sung S J, Sim J H, Kim Y I, Park S N, Jeon D H, Kim J, Hwang D K, Jeon C W, Nam D, Cheong H, Kang J K and Kim D H 2016 *J. Mater. Chem. A* **4** 10151
[4] Weber A, Krauth H, Perlt S, Schubert B, Kotschau I, Schorr S and Schock H W 2009 *Thin Solid Films* **517** 2524
[5] Tanaka T, Yoshida A, Saiki D, Saito K, Guo Q, Nishio M and Yamaguchi T 2010 *Thin Solid Films* **518** S29
[6] Zhao D D, Tian Q W, Zhou Z J, Wang G, Meng Y N, Kou D X, Zhou W H, Pan D C and Wu S X 2015 *J. Mater. Chem. A* **3** 19263
[7] Bai B, Kou D X, Zhou W H, Zhou Z J and Wu S X 2015 *Green Chem.* **17** 4377
[8] Chen H L, Kou D X, Chang Z X, Zhou W H, Zhou Z J and Wu S X 2014 *ACS Appl. Mater. Inter.* **6** 20664
[9] Fu J, Tian Q W, Zhou Z J, Kou D X, Meng Y N, Zhou W H and Wu S X 2016 *Chem. Mater.* **28** 5821
[10] Kim J, Hiroi H, Todorov T K, Gunawan O, Kuwahara M, Gokmen T, Nair D, Hopstaken M, Shin B, Lee Y S, Wang W, Sugimoto H and Mitzi D B 2014 *Adv. Mater.* **26** 7427
[11] Wang G, Zhao W G, Cui Y, Tian Q W, Gao S, Huang L J and Pan D C 2013 *ACS Appl. Mater. Inter.* **5** 10042
[12] Xin H, Katahara J K, Braly I L and Hillhouse H W 2014 *Adv. Energy Mater.* **4** 1301823
[13] Cao Y Y, Denny M S, Caspar J V, Farneth W E, Guo Q J, Ionkin A S, Johnson L K, Lu M J, Malajovich I, Radu D, Rosenfeld H D, Choudhury K R and Wu W 2012 *J. Am. Chem. Soc.* **134** 15644
[14] Zhou H P, Hsu W C, Duan H S, Bob B, Yang W B, Song T B, Hsu C J and Yang Y 2013 *Energ. Environ. Sci.* **6** 2822
[15] Wu W, Cao Y Y, Caspar J V, Guo Q J, Johnson L K, Malajovich I, Rosenfeld H D and Choudhury K R 2014 *J. Mater. Chem. C* **2** 3777
[16] Guo J, Zhou W H, Pei Y L, Tian Q W, Kou D X, Zhou Z J, Meng Y N and Wu S X 2016 *Sol. Energ. Mat. Sol. C* **155** 209
[17] Pei Y L, Guo J, Kou D X, Zhou W H, Zhou Z J, Tian Q W, Meng Y N and Wu S X 2017 *Sol. Energ.* **148** 157
[18] Ahmed S, Reuter K B, Gunawan O, Guo L, Romankiw L T and Deligianni H 2012 *Adv. Energ. Mater.* **2** 253
[19] Lei Y, Jia H M, He W W, Zhang Y G, Mi L W, Hou H W, Zhu G S and Zheng Z 2012 *J. Am. Chem. Soc.* **134** 17392
[20] Guo Q J, Ford G M, Yang W C, Hages C J, Hillhouse H W and Agrawal R 2012 *Sol. Energ. Mat. Sol.* **105** 132
[21] Kim I, Kim K, Oh Y, Woo K, Cao G, Jeong S and Moon J 2014 *Chem. Mater.* **26** 3957
[22] Ford G M, Guo Q, Agrawal R and Hillhouse H W 2011 *Chem. Mater.* **23** 2626
[23] Hages C J, Levcenco S, Miskin C K, Alsmeier J H, Abou-Ras D, Wilks R G, Bar M, Unold T and Agrawal R 2015 *Prog. Photovol.* **23** 376
[24] Giraldo S, Neuschitzer M, Thersleff T, Lopez-Marino S, Sanchez Y, Xie H B, Colina M, Placidi M, Pistor P, Izquierdo-Roca V, Leifer K, Perez-Rodriguez A and Saucedo E 2015 *Adv. Energ. Mater.* **5** 1501070
[25] Collord A D and Hillhouse H W 2016 *Chem. Mater.* **28** 2067
[26] Bag S, Gunawan O, Gokmen T, Zhu Y and Mitzi D B 2012 *Chem. Mater.* **24** 4588
[27] Khadka D B and Kim J 2015 *J. Phys. Chem. C* **119** 1706
[28] Todorov T K, Tang J, Bag S, Gunawan O, Gokmen T, Zhu Y and Mitzi D B 2013 *Adv. Energ. Mater.* **3** 201200348